

# Novel Liquid Equilibrium Valving on Centrifugal Microfluidic CD Platform\*

Wisam Al-Faqheri, *Student Member, IEEE*, Fatimah Ibrahim, *Member, IEEE*, Tzer Hwai Gilbert Thio, Hamzah Arof, Marc Madou, *Member, IEEE*

**Abstract**— One of the main challenges faced by researchers in the field of microfluidic compact disc (CD) platforms is the control of liquid movement and sequencing during spinning. This paper presents a novel microfluidic valve based on the principle of liquid equilibrium on a rotating CD. The proposed liquid equilibrium valve operates by balancing the pressure produced by the liquids in a source and a venting chamber during spinning. The valve does not require external forces or triggers, and is able to regulate burst frequencies with high accuracy. In this work, we demonstrate that the burst frequency can be significantly raised by making just a small adjustment of the liquid height in the vent chamber. Finally, the proposed valve ng method can be used separately or

combined with other valving methods in advance microfluidic processes.

## I. INTRODUCTION

In the last few decades, many researchers have focused on the study of centrifugal microfluidic CD platforms. Many of these researchers were attracted to this area of research due to the advantages of the platform such as portability, disposability and the reduced sample size required for assays implementation [1, 2]. Moreover, in comparison to the microfluidic chip, centrifugal microfluidic CD platforms do not require external pumping or mechanical actuation for liquid flow control. The platform exploits the centrifugal force generated during spinning to move fluids through the micro features on the CD.

Many microfluidic processes such as siphoning, mixing, particles separation, heating and flow switching have been performed successfully on centrifugal microfluidic CD platforms [1-3]. In recent years, many applications have also been developed on the microfluidic CD platform. Some examples include the application of Enzyme-Linked-Immunoassay (ELISA) for dengue detection [4], DNA purification [5], polymerase chain reactions (PCR) [6], and plasma separation [7].

On the microfluidic CD platform, the two main forces that control the pumping and stopping of liquid flow are the centrifugal force and the capillary force. During the spinning process, the centrifugal force ( $P_{centrifugal}$ ) pushes liquids toward the outer ring of the CD [1-3]. This force can be calculated by the following equation [1, 8]

$$P_{centrifugal} = \rho \omega^2 \Delta r \bar{r} \quad (1)$$

Where  $\rho$  is the density of the liquid,  $\omega$  is the rotational speed of the CD in radians per second (rads-1),  $\Delta r$  is the difference between the top and bottom of the liquid levels at rest with respect to the center of the CD, and  $\bar{r}$  is the average distance of the liquid from the CD center.

During the spinning of the CD, the instance when the centrifugal force (which pushes the liquid towards the CD edge) overcomes the capillary force (which prevents the liquid from moving), the liquid will burst out of the source chamber. The spinning speed where the liquid bursting happens is known as burst frequency. This spinning speed is calculated using the following equation [8]:

$$rpm = \omega \times \frac{30}{\pi} = \sqrt{\frac{P_{centrifugal}}{\rho \Delta r \bar{r}}} \left( \frac{30}{\pi} \right) \quad (2)$$

\* This research is financially supported by University of Malaya, Ministry of Higher Education High Impact Research (UM/HR/MOHE/ENG/05), and University of Malaya Research Grant (UMRG: RG023/09AET). The authors would like to acknowledge Prof. Dr. Noorsaadah Abd Rahman from Department of Chemistry, Faculty of Science, University of Malaya and her grant "Hits-to-Lead: Designing Dengue Virus Inhibitors, National Biotechnology Directorate (NBD) Initiative-Malaysian Institute of Pharmaceuticals and Nutraceuticals (IPharm), Ministry of Science, Technology and Innovation (MOSTI IPHARM 53-02-03-1049)" for partially sponsoring the initial set-up of the CD Spin Test System. Marc Madou acknowledges support of National Institute of Health (grant 1 R01 AI089541-01), and support of WCU (World Class University) program (R32-2008-000-20054-0) through the National Research Foundation of Korea funded by the Ministry of Education, Science and Technology.

Wisam Al-Faqheri is with the Medical Informatics & Biological Micro-electro-mechanical Systems (MIMEMS) Specialized Laboratory, Department of Biomedical Engineering, Faculty of Engineering, University of Malaya, 50603 Kuala Lumpur, Malaysia. (E-mail: wisamfakhri83@yahoo.com).

Fatimah Ibrahim is with the Medical Informatics & Biological Micro-electro-mechanical Systems (MIMEMS) Specialized Laboratory, Department of Biomedical Engineering, Faculty of Engineering, University of Malaya, 50603 Kuala Lumpur, Malaysia (Fax: 603 7967 4579; Tel: 603-7967-6818; E-mail: fatimah@um.edu.my).

Tzer Hwai Gilbert Thio is with the Medical Informatics & Biological Micro-electro-mechanical Systems (MIMEMS) Specialized Laboratory, Department of Biomedical Engineering, Faculty of Engineering, University of Malaya, 50603 Kuala Lumpur, Malaysia. He is also with the Faculty of Science, Technology, Engineering and Mathematics, Inti International University, Persiaran Perdana BBN, Putra Nilai, 71800 Nilai, Negeri Sembilan, Malaysia (E-mail: gilbert\_thio@hotmail.com).

Hamzah Arof is with the Medical Informatics & Biological Micro-electro-mechanical Systems (MIMEMS) Specialized Laboratory, Department of Biomedical Engineering, Faculty of Engineering, University of Malaya, 50603 Kuala Lumpur, Malaysia. He is also with the Department of Electrical Engineering, Faculty of Engineering, University of Malaya, 50603 Kuala Lumpur, Malaysia (E-mail: ahamzah@um.edu.my).

Marc Madou is with the Medical Informatics & Biological Micro-electro-mechanical Systems (MIMEMS) Specialized Laboratory, Department of Biomedical Engineering, Faculty of Engineering, University of Malaya, 50603 Kuala Lumpur, Malaysia. He is also with the Department of Biomedical Engineering, and Department of Mechanical and Aerospace Engineering, University of California, Irvine, Irvine, 92697, United States. (E-mail: mmadou@uci.edu)

In addition to the basic capillary valve, many types of alternative active and passive valves have been proposed and implemented on the microfluidic CD platform. In general, microfluidic valves can be defined as a component that stops (or starts) liquid movement in the microfluidic process. The two main categories of microfluidic valves are the passive and active valves [1, 9]. Passive valves can be defined as valves that control liquid movement without involving movable parts, for example capillary valves and siphon valves [10]. On the other hand, controlling liquid movement using external actuations is known as active valving, for example wax valves [10] and ice valves [6]. Both categories of valving techniques have their own advantages and disadvantages. The main advantage of the passive valve is that no external trigger or force is required to start (or stop) liquid movement. In the case of active valves, the main advantages are the possible sealing of liquid on the microfluidic CD during long period of storage [9], and the accurate control of liquid movement on the CD. However, when compared to the passive valve, one major disadvantage of active valving is the need for an external trigger or force such as the application of heat in the activation of wax valves.

In this study, we propose a novel liquid equilibrium valving technique that does not need external triggers to activate the valves. The liquid equilibrium valve operates on the principle of balancing the centrifugal force (or liquid pressure) from the source chamber and a venting chamber. In addition, this method allows for the controlling of the burst frequency accurately by making small changes in the venting chamber liquid height.

## II. METHODOLOGY

### A. Experimental Setup and CD Fabrication

In this section, we present the experimental setup and describe the CD fabrication process. Fig. 1 shows the customized CD spin test system used to conduct the experiments. The system consists of a variable speed stepper motor, a laser RPM counter, and a high speed camera to record the results.

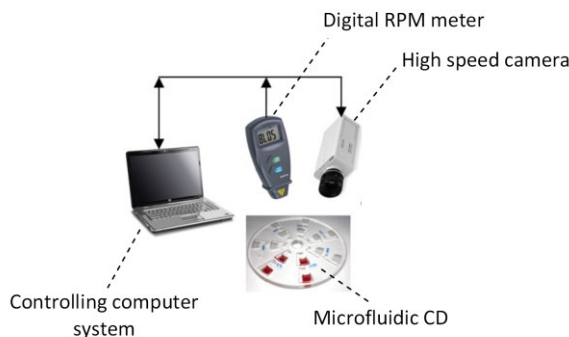


Figure 1: experimental system setup, spin test system consists of step motor, RPM meter, high speed camera, and the system is controlled by computer equipped with LabView program

The microfluidic CDs are constructed from two Polymethyl methacrylate (PMMA) discs and a sheet of custom made pressure sensitive adhesive (PSA) material (custom made by FELXcon, USA) (see Fig. 2).

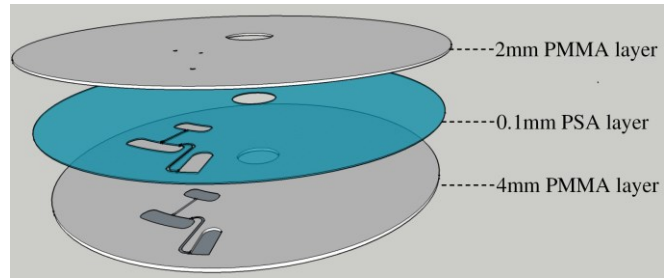


Figure 2: microfluidic CD layers, 2mm PMMA top layer, 0.1mm PSA middle layer, and 4mm PMMA bottom layer

The top PMMA disc is 2mm thick and contains only venting holes cut through the disc. The bottom PMMA disc is 4mm thick and contains engraved microfluidic process features. A Computer Numerical Control (CNC) machine (model VISION 2525, by Vision Engraving and Routing Systems, USA) is utilized to cut the venting holes and engrave the microfluidic features in the PMMA discs. The PSA sheet contains identical microfluidic process features cut using a cutter plotter (model PUMA II, by GCC, Taiwan). This ensures that the liquid sample in the microfluidic process is surrounded by uniform features to prevent the sticky material of the PSA to affect the burst frequency. The PMMA discs and the PSA sheet are bound and pressed together using a customized press roller system.

### B. Microfluidic CD Design

The CD designed for the experimental work is illustrated in Fig. 3. The design consists of a source chamber, a destination chamber, and a venting chamber (see Fig. 3). The chambers are connected by channels of dimensions 0.7mm width and 0.5mm depth. As illustrated in Fig. 3, the source chamber has two venting holes while the destination chamber is ventless and is connected to the venting chamber. This configuration creates a state of compressed-air as liquids in both the source and venting chamber is pushed radially outward towards the CD edge by the centrifugal force. This will be discussed further in detail in the “*Experimental Method*” section.

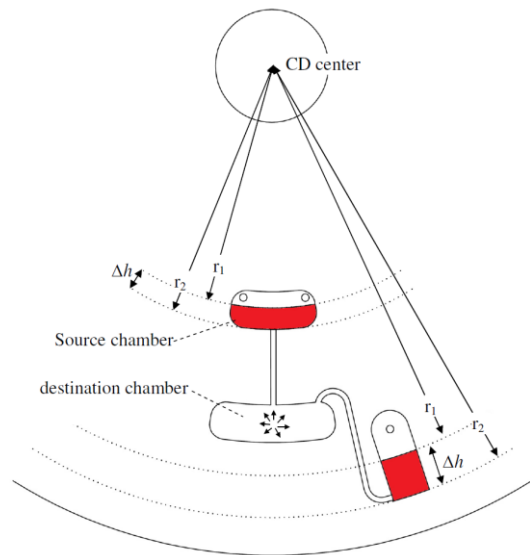


Figure 3: Liquid valve CD design: source, destination, venting chamber

The source chamber and destination chambers have a depth of 1mm and are designed to respectively each hold 40 $\mu$ l and 80 $\mu$ l of liquid. The venting chamber has a depth of 3mm and is designed to hold a maximum of 150  $\mu$ l. The big volume of the venting chamber allows for the testing of the effect of a wide range of liquid height on the burst frequency.

### C. Experimental Method

Each experiment was performed for a total of five times. A mixture of de-ionized water and color dye (at a ratio of one part dye to ten part water) was used as the test liquid in all experiments.

In every experiment, the source chamber is first loaded with 40 $\mu$ l of colored water through the venting holes. Next specified amount of colored water ranging from 0 to 50  $\mu$ l is loaded into the venting chamber to achieve a venting chamber liquid height,  $\Delta h$  ranging from 0 to 3.35 mm (see Fig. 3). As shown by equation (1), it is clear that the venting chamber liquid height,  $\Delta h$  is considered as the variable that affects burst pressure (frequency). From the venting chamber design, each 1 $\mu$ l of liquid is equivalent to a venting chamber liquid height of 0.067mm. As an example, 50 $\mu$ l of liquid in the venting chamber produces an effective liquid height,  $\Delta h$  of approximately 3.35mm.

After the source and venting chambers are loaded with liquid, the microfluidic CD is mounted on the CD spin test system and the spin speed is gradually increased. As the speed is increased, the liquid in the source chamber starts moving into the channel due to the increasing centrifugal force and finally burst into the destination chamber. The rpm as which this occurs is recorded in Fig. 5. For further comparison, the centrifugal force due to the varying venting chamber liquid height,  $\Delta h$  is calculated using equation (1). The results are included in Fig. 5.

## III. RESULTS AND DISCUSSION

### A. Operation of the Liquid Equilibrium Valve

In this section, the theoretical prediction of the operation of the liquid equilibrium valve is presented and compared to the experimental observations in Fig. 4.

For ease of discussion, we refer to the centrifugal force due to liquid from the source chamber as the source chamber liquid pressure, and we refer to the centrifugal force due to liquid from the venting chamber as the venting chamber liquid pressure.

In theory, in the initial stage at low rpm speeds, the source chamber liquid pressure is at equilibrium with (or lower than) the venting chamber liquid pressure. In this stage the air in the destination chamber is trapped by the liquids from the source and venting chambers (see Fig 4(a)). At higher spin speed, the liquid pressures from both the source and venting chambers start to exert pressure on the air within the destination chamber. This creates an air-compression state in the chamber. In this stage, liquid from source chamber starts entering the connecting channel between the source and destination chamber. This movement of liquid into the channel results in (i) compression of air, leading to an increase in the pressure inside the destination chamber (see Fig. 4(b)), and (ii) a higher source liquid pressure due to an increase in the value of  $\Delta r$  (refer to Equation (1) and Fig.

3). As the source chamber liquid pressure becomes greater than the venting chamber liquid pressure, liquid from the source chamber starts to enter the destination chamber, and the pressurized air in turn pushes liquid out of the channel connecting the destination and venting chambers. This causes the compressed air in the destination chamber to escape through the venting chamber liquid in the form of bubbles (see Fig. 4(b)). This then destabilizes the pressure barrier holding back the liquid in the source chamber, and the liquid then fully bursts from the source chamber to the destination chamber (see Fig. 4(c)).

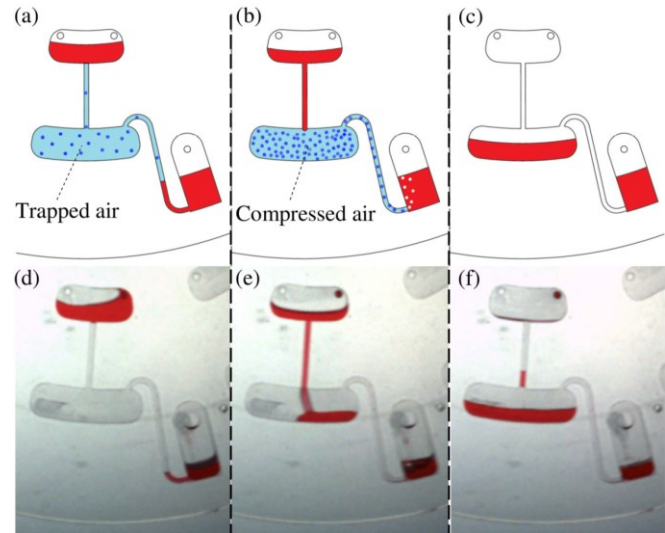


Figure 4: Liquid status during spinning process, (a) starting and low spinning frequency liquid status, (b) liquid moves inside the microchannel due to the high rpm with bubble escaping in the venting chamber, (c) liquid fully transferred to the destination chamber, (d, e, and f) are figures captured from the experimental test

The stages of the operation of the liquid equilibrium valve during experimental observations are shown in Fig 4(d-f). Fig. 4(d) shows the initial position of liquid during the low spinning speed where the source chamber liquid pressure is not sufficient to burst the liquid. As the spin speed is increased, the liquid moves into the channel and bursts into the destination chamber as shown in Fig (e and f).

The scenario in Fig. 4 represents cases where the source chamber liquid pressure is able to overcome the venting chamber liquid pressure. In cases where the liquid height,  $\Delta h$  is big and produces a liquid pressure that is greater than the source chamber liquid pressure even at high frequencies ( $\sim$ 1500rpm), the source chamber liquid will not burst.

### B. Effects of liquid height, $\Delta h$ in the venting chamber

In this section, the effects of venting chamber liquid height,  $\Delta h$  (produced by varying the volume of liquid in the venting chamber) is investigated. As indicated in the “Experimental Method” section, it is clear from equation (1) that the height of liquid is the factor that affects the venting chamber liquid pressure, and not the volume of liquid. However, because the liquid volume is limited by the pipette used for liquid loading, we fixed the volume of liquid loaded into the venting chamber to a range of 20 to 50 $\mu$ l, and calculate the resulting liquid height using a conversion factor of 0.067mm per 1 $\mu$ l of liquid.

Figure 5 presents the burst frequency for different venting chamber liquid height,  $\Delta h$ , and also the venting chamber liquid pressure in each corresponding case. The overall trend shows that increasing the liquid height,  $\Delta h$  in the venting chamber leads to an increase in burst frequency. This result is in agreement with equation (1) which shows that increasing the venting chamber liquid height will result in an increase of the venting chamber liquid pressure. A high venting chamber liquid pressure requires a high source chamber liquid pressure to overcome it. The results indicates that increasing the liquid height in the venting chamber from 0mm (0 $\mu$ l) to 3.35mm (50 $\mu$ l) increases the centrifugal pressure, which in turn increases the burst frequency from 290RPM to around 1080RPM (as indicated by equations (1) and (2)). This significantly increases the burst frequency by merely increasing the liquid height by 3.35mm. Further comparison to the venting chamber liquid pressure indicates an increase in liquid pressure when the liquid height increases. This agrees with the notion that high burst frequency is required due to the increasing source chamber liquid pressure required to overcome the venting chamber liquid pressure.

All the experimental tests were performed on a borderline hydrophobic PMMA material (contact angle around 80°). It is believed that operating the liquid equilibrium valve on highly hydrophilic material will reduce the valving ability where the liquid from the source chamber will be easier to move inside the channel and then into the destination chamber.

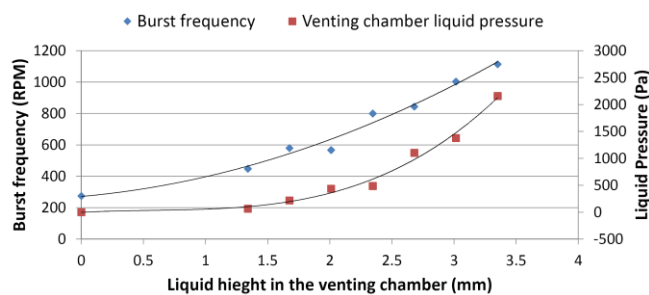


Figure 5: Burst frequency of source chamber liquid, and venting chamber liquid pressure vs. different venting chamber liquid height ( $\Delta h$ ). The solid lines are 2<sup>nd</sup> order polynomial trend lines of the burst frequency and venting chamber liquid pressure results

The experimental results indicate that the proposed liquid equilibrium valve provides high flexibility in fluid control, and an ability to increase the burst frequency by simply making small changes to the venting chamber liquid height,  $\Delta h$ . Moreover, when compared to other alternative microfluidic valves, this liquid equilibrium valve does not need external triggers or actuators to activate the valve.

#### IV. CONCLUSION

This work presents a novel liquid equilibrium microfluidic valve based on the principle of liquid pressure equilibrium. The results show that the introduced liquid equilibrium valving method has the ability to accurately control the burst frequency of the liquid on the microfluidic CD. Moreover, with just a small adjustment in the venting chamber liquid height, the burst frequency can be increased significantly. In comparison to currently available alternative microfluidic passive and active valves, the proposed valve does not need any external trigger to active it. In addition, there is no

contact between the liquid in the valve and the samples on the CD. The presented valve can be used independently or combined with other valves in complex and advance process. Finally, the developed valve can be implemented in biomedical or clinical processes as no external trigger such as heating source is required. Moreover, in comparison to the previously proposed active valve, there is no contamination of the sample by the valving material.

#### REFERENCES

- [1] M. Madou, J. Zoval, G. Jia, H. Kido, J. Kim, and N. Kim, "Lab on a CD," *Annual Review of Biomedical Engineering* 8, vol. 8, pp. 601-628, 2006.
- [2] J. V. Zoval and M. J. Madou, "Centrifuge-based fluidic platforms," *Proceedings of the IEEE*, vol. 92, pp. 140-153, 2004.
- [3] J. Ducrée, S. Haeberle, S. Lutz, S. Pausch, F. Von Stetten, and R. Zengerle, "The centrifugal microfluidic Bio-Disk platform," *Journal of Micromechanics and Microengineering*, vol. 17, pp. S103-S115, 2007.
- [4] F. Ibrahim, A. A. Nozari, P. Jahanshahi, N. Soin, N. A. Rahman, S. Z. M. Dawal, M. K. B. A. Kahar, K. A. Samra, and M. Madou, "Analysis and experiment of centrifugal force for microfluidic ELISA CD platform," in *Proceedings of the IEEE Conference on Biomedical Engineering and Sciences (IECBES)*, Kuala Lumpur, 2010, pp. 466-470. DOI 10.1109/IECBES.2010.5742282
- [5] O. Strohmeier, A. Emperle, G. Roth, D. Mark, R. Zengerle, and F. von Stetten, "Centrifugal gas-phase transition magnetophoresis (GTM)—a generic method for automation of magnetic bead based assays on the centrifugal microfluidic platform and application to DNA purification," *Lab on a Chip*, 2013.
- [6] M. Amasia, M. Cozzens, and M. J. Madou, "Centrifugal microfluidic platform for rapid PCR amplification using integrated thermoelectric heating and ice-valving," *Sensors and Actuators, B: Chemical*, vol. 161 (1), pp. 1191-1197, 2012.
- [7] B. S. Lee, J. N. Lee, J. M. Park, J. G. Lee, S. Kim, Y. K. Cho, and C. Ko, "A fully automated immunoassay from whole blood on a disc," *Lab Chip*, vol. 9, pp. 1548-1555, 2009.
- [8] T. H. G. Thio, S. Soroori, F. Ibrahim, W. Al-Faqheri, N. Soin, L. Kulinsky, and M. Madou, "Theoretical development and critical analysis of burst frequency equations for passive valves on centrifugal microfluidic platforms," *Medical & Biological Engineering & Computing*, 2013 DOI 10.1007/s11517-012-1020-7
- [9] T. Thio, A. A. Nozari, N. Soin, M. K. B. A. Kahar, S. Z. M. Dawal, K. A. Samra, M. Madou, and F. Ibrahim, "Hybrid Capillary-Flap Valve for Vapor Control in Point-of-Care Microfluidic CD," in *5th Kuala Lumpur International Conference on Biomedical Engineering 2011*, vol. 35, N. Osman, W. Abas, A. Wahab, and H.-N. Ting, Eds., ed: Springer Berlin Heidelberg, 2011, pp. 578-581.
- [10] K. Abi-Samra, R. Hanson, M. Madou, and R. A. Gorkin III, "Infrared controlled waxes for liquid handling and storage on a CD-microfluidic platform," *Lab Chip*, vol. 11, pp. 723-726, 2011.